Eur. Phys. J. C (2025) 85:953
https://doi.org/10.1140/epjc/s10052-025-14660-6

THE EUROPEAN PHYSICAL JOURNAL C

Regular Article - Theoretical Physics

Circular motion and collisions of charged spinning test particles around magnetized Schwarzschild black hole

Tursinbay Oteev[1,2,a], **Zdeněk Stuchlík**[3,b], **Javlon Rayimbaev**[4,5,c], **Inomjon Ibragimov**[6,d], **Murat Sharibaev**[2,e], **Ahmadjon Abdujabbarov**[7,8,9,f]

[1] Nukus State Pedagogical Institute, Seyitov St. 104, 230100 Nukus, Uzbekistan
[2] Karakalpak State University, Sh.Abdirov 1, 230112 Nukus, Uzbekistan
[3] Research Centre for Theoretical Physics and Astrophysics, Institute of Physics, Silesian University in Opava, Bezručovo nám. 13, 74601 Opava, Czech Republic
[4] New Uzbekistan University, Movarounnahr Str. 1, 100000 Tashkent, Uzbekistan
[5] Institute of Theoretical Physics, National University of Uzbekistan, 100174 Tashkent, Uzbekistan
[6] Kimyo International University in Tashkent, Shota Rustaveli street 156, 100121 Tashkent, Uzbekistan
[7] School of Physics, Harbin Institute of Technology, Harbin 150001, People's Republic of China
[8] University of Tashkent for Applied Sciences, Str. Gavhar 1, 100149 Tashkent, Uzbekistan
[9] Tashkent State Technical University, 100095 Tashkent, Uzbekistan

Received: 6 July 2025 / Accepted: 12 August 2025

Abstract The study of spinning charged particle dynamics around black holes in external fields offers insights into relativistic motion and the influence of spin-curvature and electromagnetic interactions. In this work, we investigate the motion of spinning charged test particles in the vicinity of Schwarzschild black holes immersed in asymptotically uniform magnetic fields. Using the Mathisson–Papapetrou–Dixon (MPD) equations, we derive the equations of motion and analyze the superluminal bound, which constrains the physically admissible values of the spin parameter. We investigate how this bound depends on the magnetic interaction parameter ω, which couples the particle's charge to the external magnetic field. Furthermore, we explore the effective potential and examine how both spin and ω affect circular orbits and the dynamics of the particle. Our results reveal the nonlinear interplay between spin, curvature, and magnetic interaction, contributing to the broader understanding of charged spinning test particle motion in magnetized relativistic environments.

[a] e-mail: oteevtp@gmail.com
[b] e-mail: zdenek.stuchlik@fpf.slu.cz
[c] e-mail: javlon@astrin.uz (corresponding author)
[d] e-mail: i.ibragimov@kiut.uz
[e] e-mail: sharibaev.m.b@gmail.com
[f] e-mail: ahmadjon@astrin.uz

1 Introduction

Extreme mass ratios in astrophysical scenarios, as observed in the galactic center, permit an approximate analytic description of the motion under specific parameter restrictions. The steadily improving observational situation of the galactic center [1–3] may soon enable us to test various competing theoretical approaches to model the motion of astrophysical objects within the framework of General Relativity. This work aims to study the motion of spinning charged particles in the presence of magnetic and gravitational fields.

The motion of spinning test particles was studied for the first time by Mathisson in 1937 when he considered the problem of extended bodies in general relativity(GR) [4]. Later, Papapetrou, Tulczyjew, Moller, and others improved the Mathisson methods [5–16]. Today, the equations that describe the motion of extended bodies with spin and mass are known as MPD equations. Recently, the authors derived the equations of motion for spinning test particles using the MPD equations and the Tulczyjew spin-supplementary condition [17,18]. Various features of spinning test particle motion have been investigated for different backgrounds by other authors [19–28].

There is convincing evidence that magnetic fields are indeed present near black holes. Observations of the Galactic center [29] have demonstrated the existence of strong magnetic fields of hundreds of Gauss in the vicinity of the supermassive black hole (SMBH) at the Galactic center. In March

Published online: 08 September 2025

of this year, the Event Horizon Telescope (EHT) collaboration, a global research team, has captured the first-ever view of polarized light and the magnetic fields that surround Sagittarius A* (Sgr A*), the supermassive black hole at the heart of the Milky Way [30,31]. Therefore, this historic EHT observation of Sgr A* suggests that strong and well-organized magnetic fields could be common to all black holes.

Analytical expressions offer two advantages. Firstly, they provide a basis for numerical methods, thereby facilitating comprehensive exploration of the parameter space for predicting astrophysical observables. Secondly, they can be used as benchmarks for numerical methods. A brief reference to find exact analytical solutions for geodesic equations of particles is given in the work [32] recently. These methods, which are based on the theories of elliptic functions and modular forms, were studied by brilliant mathematicians of the nineteenth century, including Jacobi [33], Abel [34], Riemann [35,36], and Weierstrass [37]. For further details, please see Ref. [38], which comprehensively reviews these discoveries. Notably, modular forms have been applied to solve (hyper-)elliptic integrals involved in particle trajectory studies, which has attracted significant attention in recent decades. These methods, which are rooted in the theories of elliptic functions and modular forms, have been the focus of numerous investigations analyzing trajectory curves in black hole spacetimes [39–55].

Building upon this scientific foundation, contemporary research continues to explore the properties and dynamics of particles falling in gravitational fields in diverse astrophysical contexts. Bound and unbound particle orbits are of particular interest, as they represent fundamental aspects of motion and offer valuable insights into the structure and evolution of the universe. Bound orbits, characterized by closed trajectories around central masses, are found extensively in celestial systems. These include planetary orbits in the solar system and the motion of stars in galaxies [56,57]. These orbits contribute to the stability and long-term dynamics of astrophysical objects. They also provide essential constraints on theoretical gravitational dynamics and models of cosmological evolution. Recent studies have examined related problems for charged spinning particles in various field configurations [58].

In this manuscript, we study the motion of charged spinning test particles around a magnetized Schwarzschild black hole. In particular, we analyze the influence of spin–curvature coupling and magnetic interactions on circular motion and particle collisions. In Sect. 2, we formulate the theoretical framework by introducing the modified Mathisson–Papapetrou–Dixon (MPD) equations in the presence of an external magnetic field and derive key conserved quantities. We also obtain analytical expressions for the effective potential and establish the conditions for timelike motion (superluminal bound). In Sect. 3, we explore the effects of spin and magnetic interaction on the effective potential and study the behavior of the innermost stable circular orbits (ISCOs). In Sect. 5, we examine high-energy collisions between charged spinning particles and analyze how spin and magnetic coupling affect the center-of-mass energy. Finally, in Sect. 5, we summarize our findings and highlight their physical implications. Throughout the paper, we adopt geometrized units with $G_0 = c = 1$ and use dimensionless quantities.

2 Test spinning charged particle motion

In this section, we derive the equations of motion governing charged spinning test particles orbiting a Schwarzschild black hole in the presence of an externally applied asymptotically uniform magnetic field. The line element describing the exterior spacetime of a Schwarzschild black hole with mass M is given by

$$ds^2 = -f(r)dt^2 + f(r)^{-1}dr^2 + r^2 d\Omega^2, \tag{1}$$

in the usual Schwarzschild coordinates $x^\alpha = (t, r, \theta, \varphi)$, with $d\Omega^2 = d\theta^2 + \sin\theta^2 d\varphi^2$, where the lapse function is given by

$$f(r) = 1 - \frac{2M}{r}. \tag{2}$$

2.1 Magnetized Schwarzschild black holes

The classical Wald solution [59] for the electromagnetic four-potential of the external asymptotically uniform electromagnetic field around the Schwarzschild black hole has the form,

$$A_\varphi = \frac{1}{2} B_0 r^2 \sin^2\theta \tag{3}$$

the asymptotic value of the magnetic field is B_0. The non-zero components of the electromagnetic tensor ($F_{\mu\nu} = A_{\nu,\mu} - A_{\mu,\nu}$) are

$$F_{r\varphi} = B_0 r \sin^2\theta \tag{4}$$

$$F_{\theta\varphi} = B_0 r^2 \sin\theta\cos\theta \tag{5}$$

and non-zero components of the magnetic fields around the Schwarzschild BH are calculated as,

$$B^\alpha = \frac{1}{2}\eta^{\alpha\beta\sigma\mu} F_{\beta\sigma} w_\mu \tag{6}$$

where, w_μ is the four-velocity of the proper observer, $\eta_{\alpha\beta\sigma\gamma}$, is the pseudo-tensorial form of the Levi-Civita symbol, and it has the following relations:

$$\eta_{\alpha\beta\sigma\gamma} = \sqrt{-g}\epsilon_{\alpha\beta\sigma\gamma} \quad \eta^{\alpha\beta\sigma\gamma} = -\frac{1}{\sqrt{-g}}\epsilon^{\alpha\beta\sigma\gamma}. \tag{7}$$

Here g is the determinant of the spacetime metric, and it is for the Schwarzschild case $g = -r^4\sin^2\theta$, and the Levi-

Civita symbol $\epsilon_{0123} = 1$ for the even permutations, and for odd ones -1.

The orthonormal components of the magnetic fields can be expressed using the electromagnetic field tensor in the following form:

$$B^{\hat{i}} = \frac{1}{2}\epsilon_{ijk}\sqrt{g_{jj}g_{kk}}F^{jk} = \frac{1}{2}\epsilon_{ijk}\sqrt{g^{jj}g^{kk}}F_{jk} \tag{8}$$

Consequently, the radial and vertical components of the magnetic field measured by Zero Angular Momentum Observer (ZAMO) with the velocities $v^{\mu}_{ZAMO} = (1/\sqrt{f(r)}, 0, 0, 0)$ take the form,

$$B^{\hat{r}} = B_0\cos\theta, \quad B^{\hat{\theta}} = \sqrt{f(r)}B_0\sin\theta. \tag{9}$$

2.2 The effective potential for a charged spinning particle's motion

The effects of external magnetic fields in test-charged particle's dynamics play a crucial role. The motion and radiation of charged particles around a magnetized black hole, taking into account radiation reaction forces, have been extensively studied in Refs. [60,61]. Additionally, studies on the motion of magnetized particles around black holes in the presence of external magnetic fields, along with the spin effects, hold promise for an interesting future in their dynamics.

In this paper, we first investigate the dynamics of the spinning charged test particle orbiting a magnetized Schwarzschild black hole. The equations of motion of spinning particles can not be described by the geodesic equation in general relativity due to the presence of gravitational coupling between the Riemann curvature tensor and the spin of the orbiting particle in the black hole spacetime [4–6,62].

The equations of motion for a charged spinning test particle around a magnetized black hole are given by a modification of the MPD equations, including the force due to the gauge field. Indeed, there is a magnetic moment of spinning charge. However, we consider this moment negligible and attribute the electromagnetic interaction to the Lorentz force exerted by the surrounding magnetic field and the charge of the spinning particle. This approximation is consistent with the linear-in-spin framework employed in our analysis, where magnetic dipole terms of the form $\mu^{\alpha\beta}F_{\alpha\beta}$ are of higher order and thus neglected, as also done in Refs. [63–65]. Then, the system reads with the electromagnetic interaction term [66].

$$\frac{Dp^{\alpha}}{d\lambda} = -\frac{1}{2}R^{\alpha}_{\beta\rho\sigma}v^{\beta}S^{\rho\sigma} - mqF^{\alpha}_{\beta}v^{\beta}, \tag{10}$$

$$\frac{DS^{\alpha\beta}}{d\lambda} = p^{\alpha}v^{\beta} - v^{\alpha}p^{\beta}, \tag{11}$$

where $D/d\lambda$ is the projection of the covariant derivative along the particle's trajectory, $v^{\alpha} = dx^{\alpha}/d\lambda$ is the 4-velocity of the test particle, p^{α} is the canonical 4-momentum, q is test particle's electric charge, m corresponds to the dynamical rest mass defined by $m^2 = -p_{\alpha}p^{\alpha}$, $R^{\alpha}_{\beta\sigma\delta}$ is the Riemann curvature tensor, and λ is an affine parameter. The second-rank tensor $S^{\alpha\beta}$ is antisymmetric $S^{\alpha\beta} = -S^{\beta\alpha}$. Eq. (10) determines the coupling between the Riemann tensor $R^{\alpha}_{\mu\rho\sigma}$, and spin of the particle. To see this coupling, let us consider the well-known geodesic equation in GR,

$$v^{\beta}\partial_{\beta}v^{\alpha} + \Gamma^{\alpha}_{\sigma\beta}v^{\sigma}v^{\beta} = 0. \tag{12}$$

In terms of the particle's 4-momentum and the projection of the covariant derivative along the particle's trajectory, Eq. (12 can be expressed in the form,

$$\frac{Dp^{\alpha}}{d\lambda} = 0. \tag{13}$$

Therefore, comparing Eqs. (10) and (13), one can see how the interaction between the Riemann curvature tensor and the antisymmetric tensor $S^{\alpha\beta}$ affects the motion of spinning test particles in curved spacetime.

A crucial aspect of the MPD equations is related to the center of mass of the spinning particle. In this sense, to solve the system in Eqs. (10) and (11), one has to fix its center of mass. This assumption is made by including condition [7,67]

$$S^{\alpha\beta}p_{\alpha} = 0. \tag{14}$$

The condition (14) is known as the Tulczyjew spin supplementary condition (SSC) [68]. Among several SSCs, we adopt the Tulczyjew condition $S^{\alpha\beta}p_{\beta} = 0$, which fixes the center-of-mass worldline by requiring spin to be orthogonal to the particle's momentum. This SSC is commonly used in studies of spinning particles because of its simplicity and well-posed behavior in the linear-in-spin regime. Although alternative SSCs exist, such as the Mathisson–Pirani and Ohashi–Kyrian–Semerák conditions, and may lead to different physical predictions, particularly in strong-field regions, we restrict our analysis to the Tulczyjew SSC for consistency with previous literature [69,70]. From Eq. (14), the canonical momentum and the spin of the particle provide two independent conserved quantities given by the relations

$$p^{\alpha}p_{\alpha} = -m^2, \tag{15}$$

$$S^{\alpha\beta}S_{\alpha\beta} = 2S^2 = 2m^2s^2. \tag{16}$$

Nevertheless, in contrast to the spinning test particle's canonical momentum conservation, it is important to point out that the squared velocity does not necessarily satisfy the condition,

$$v_{\alpha}v^{\alpha} = -1, \tag{17}$$

because the 4-vectors p^{α} and v^{α} are not always parallel. In this sense, to ensure that the particle's 4-velocity is always smaller than the speed of light, one must impose an additional condition: *the superluminal bound* (see Sect. 2.3).

In addition to the conserved quantities resulting from the Tulczyjew SSC condition, one also has the conserved quantities associated with the spacetime symmetries. There are the usual background-dependent conserved quantities associated with the Killing vectors, k^α, which can be expressed as: [24]

$$C_k = p^\alpha k_\alpha - \frac{1}{2} S^{\alpha\beta} \nabla_\beta k_\alpha + mqk^\alpha A_\alpha. \tag{18}$$

In fact, the charged particle interacts with only the external magnetic field that does not break the conservative quantities p_t and p_ϕ of spinning particles, and they can be obtained from Eq. (18) as:

$$-E = p_t - \frac{1}{2} g_{t\alpha,\beta} S^{\alpha\beta} = p_t - \frac{1}{2} g_{tt,r} S^{tr}, \tag{19}$$

$$J = p_\varphi - \frac{1}{2} g_{\varphi\alpha,\beta} S^{\alpha\beta} + mqA_\varphi \tag{20}$$

$$= p_\varphi + \frac{1}{2} g_{\varphi\varphi,r} S^{r\varphi} + \frac{1}{2} mqB_0 r^2 \sin\theta^2, \tag{21}$$

where J is the total angular momentum of the spinning particle; therefore, it can be described as the sum of angular momentum due to rotation and the absolute value of spin, $J = L + S$. At this point, it is convenient to divide both sides of the last two equations by mass m and work with quantities per unit of mass. Thus, we introduce the following denotations $\mathcal{E} = E/m$, $\mathcal{J} = J/m$, $\mathcal{L} = L/m$, $s = S/m$, $u_\alpha = p_\alpha/m$ and $\omega = qB_0$. Here ω represents the interaction between a magnetic field and a charge. We restrict our investigation to an equatorial plane where $\theta = \pi/2$. Taking into account the introduced denotations, we rewrite the Eqs. (19) and (21)

$$-\mathcal{E} = u_t - \frac{1}{2m} g_{t\alpha,\beta} S^{\alpha\beta} = u_t - \frac{1}{2m} g_{tt,r} S^{tr}, \tag{22}$$

$$\mathcal{J} = u_\varphi + \frac{1}{2m} g_{\varphi\varphi,r} S^{r\varphi} + \frac{1}{2}\omega r^2. \tag{23}$$

From Eq. (14) we find the following equalities:

$$S^{t\phi} = -\frac{p_r}{p_\phi} S^{tr}, \quad S^{r\varphi} = \frac{p_t}{p_\phi} S^{tr}. \tag{24}$$

Using the Eqs. (15), (16) and (24) conditions one may get the equations below:

$$S^{tr} = \frac{s}{\sqrt{-g_{tt} g_{rr} g_{\varphi\varphi}}} p_\varphi, \quad S^{r\varphi} = \frac{s}{\sqrt{-g_{tt} g_{rr} g_{\varphi\varphi}}} p_t. \tag{25}$$

As mentioned before, we explore the motion of spinning charged particles on the equatorial plane. Hence, one may write the polar component of the Schwarzschild metric tensor as $g_{\varphi\varphi} = r^2$. Further taking into account that $g_{tt} = -f(r)$ and $g_{rr} = 1/f(r)$ one may the last equations in the simple form:

$$S^{tr} = \frac{s}{r} p_\varphi, \quad S^{r\varphi} = \frac{s}{r} p_t. \tag{26}$$

Now he Eqs. (22) and (23) can be described as:

$$-\mathcal{E} = u_t - \frac{s u_\varphi}{2r} g_{tt,r}, \tag{27}$$

$$\mathcal{J} = u_\varphi + \frac{s u_t}{2r} g_{\varphi\varphi,r} + \frac{1}{2}\omega r^2 \tag{28}$$

and solving the Eqs. (27) and (28) we get:

$$u_t = -\frac{2\mathcal{E}r^3 + 2\mathcal{J}s - r^2 s\omega}{2\left(r^3 - s^2\right)}, \tag{29}$$

$$u_\varphi = \frac{r^3\left(2\mathcal{E}s + 2\mathcal{J} - r^2\omega\right)}{2\left(r^3 - s^2\right)}, \tag{30}$$

here we considered the mass of the Schwarzschild black hole equal to one, $M = 1$. So the lapse function takes the form $f(r) = 1 - 2/r$.

Now, we rewrite Eq. (15), dividing both sides by m^2 in the following form $u^\alpha u_\alpha = -1$, and get the equation for the effective potential of the spinning charged particle,

$$(u^r)^2 = \frac{\rho}{\sigma}(\mathcal{E}^2 + \delta\mathcal{E} + \gamma) \tag{31}$$

where

$$\rho = r^3\left(r^3 - rs^2 + 2s^2\right),$$

$$\sigma = \left(r^3 - s^2\right)^2, \quad \delta = \frac{(r-3)s\left(r^2\omega - 2\mathcal{J}\right)}{r^3 - (r-2)s^2},$$

$$\gamma = \frac{1}{4r^7 - 4(r-2)r^4 s^2}\Big(4\mathcal{J}^2 r\left(s^2 - (r-2)r^3\right) + 4\mathcal{J}r^3\omega\left((r-2)r^3 - s^2\right) - 4(r-2)\left(r^3 - s^2\right)^2 + r^5\omega^2\left(s^2 - (r-2)r^3\right)\Big).$$

We may rewrite Eq. (31) as,

$$(u^r)^2 = \frac{\rho}{\sigma}(\mathcal{E} - V_+)(\mathcal{E} - V_-) \tag{32}$$

Therefore, it is possible to define the effective potential for the circular motion of the spinning magnetized particles $u^r = 0$ as a solution of Eq. (32) in the following form [24].

$$V_\pm = \frac{-\delta \pm \sqrt{\delta^2 - 4\gamma}}{2} \tag{33}$$

One can see from Eq. (32) that to have $(u_r)^2 \geq 0$, the specific energy of the test particles has to satisfy the conditions: (i) $\mathcal{E} < V_-$ or (ii) $\mathcal{E} > V_+$.

Hence, we focus on the case of spinning test particles with positive energy, which coincides with the effective potential being $V_{\rm eff} = V_+$. Here we redefine the effective potential as,

$$V_{eff} = \frac{-\delta + \sqrt{\delta^2 - 4\gamma}}{2} \tag{34}$$

We now analyze the effects of spin and magnetic interactions, as well as their combined effects on the effective potential for the radial motion of test spinning and magnetized particles graphically, due to the complicated form of the potential expression.

2.3 Superluminal bound

This subsection investigates the superluminal limit, a condition essential for determining the permissible values of s that ensure a spinning test particle follows a physically meaningful trajectory. Accordingly, we derive analytical expressions for static and spherically symmetric spacetimes. Then, in Sect. 3, we apply these formulas to the specific case of a Schwarzschild black hole immersed in an externally applied, asymptotically uniform magnetic field.

As previously noted, although the condition $p_\alpha p^\alpha = -m^2$ is satisfied, the normalization $v_\alpha v^\alpha = -1$ does not necessarily hold, since the four-momentum and four-velocity are not generally aligned. Consequently, as the spinning test particle approaches the center of symmetry, the magnitude of the four-velocity v^α increases, and for certain values of the spin s and radial coordinate, some components of v^α may diverge. In this scenario, the particle's motion transitions from a time-like to a space-like trajectory, indicating a superluminal bound.

Particles following spacelike trajectories (i.e., exhibiting superluminal motion) lack physical interpretation within the framework of general relativity. Therefore, the transition to $v_\alpha v^\alpha > 0$ is forbidden for physically realistic particles. To prevent this unphysical behavior, an additional constraint must be imposed, referred to as the *superluminal bound*, which requires that $v_\alpha v^\alpha < 0$. To ensure that spinning test particles remain on physically admissible (timelike) trajectories, we impose the following condition [18,71]:

$$\frac{v_\alpha v^\alpha}{(v^t)^2} = g_{tt} + g_{rr}\left(\frac{dr}{dt}\right)^2 + 2g_{t\varphi}\frac{d\varphi}{dt} + g_{\varphi\varphi}\left(\frac{d\varphi}{dt}\right)^2 < 0. \tag{35}$$

To incorporate this superluminal bound into our analysis, we require explicit expressions for dr/dt and $d\varphi/dt$. For this purpose, we follow the method introduced by Hojman and Asenjo in Ref. [72]. As in our previous works [25,28], we constrain the motion to the equatorial plane ($\theta = \pi/2$), where the nonvanishing components of the spin tensor $S^{\alpha\beta}$ are S^{tr}, $S^{t\varphi}$, and $S^{r\varphi}$. Since the full derivation of the expressions for dr/dt and $d\varphi/dt$ under this condition is already provided in Refs. [25,28], we do not repeat it here.

Using these expressions for dr/dt and $d\varphi/dt$, we evaluate the superluminal condition as a function of the spin parameter s and the interaction parameter ω, which characterizes the coupling between the external magnetic field and the charge. This allows us to ensure that any given value of s lies within the domain of physical motion, the region where the trajectory remains timelike.

To illustrate this, Fig. 1 shows the (ω, s)-plane with shaded regions corresponding to $v_\alpha v^\alpha < 0$. These areas define the range of spin values that preserve causality and physical consistency. The boundary of the shaded region delineates the critical values beyond which the motion becomes superluminal and hence unphysical. The curve forming this boundary is generally smooth and continuous, but its steepness increases significantly for large spin magnitudes, especially near the limits of the shaded domain. This behavior reflects the strong sensitivity of the superluminal condition to both the spin parameter s and the magnetic coupling ω. Notably, the curve tends to flatten near $\omega = 0$, indicating that magnetic interaction becomes less relevant in the absence of field coupling. This analysis offers insight into the nonlinear interplay between spin, geometry, and magnetic interaction in curved spacetime.

3 Dynamics of charged spinning test particles around magnetized Schwarzschild black hole

3.1 Effective potential

We consider all possible configurations of a charged spinning test particle orbiting a Schwarzschild black hole immersed in an asymptotically uniform external magnetic field. Figure 2 illustrates the radial profiles of the effective potential $V_{\rm eff}$ for a spinning test particle in the spacetime of a magnetized Schwarzschild black hole, for various values of the spin parameter s and the magnetic coupling parameter ω.

The left panel in Fig. 2 shows the effective potential as a function of the radial coordinate r for a fixed angular momentum $\mathcal{L} = 4$ and magnetic coupling parameter $\omega = 0.01$, while varying the spin s from -0.8 to 0.8. The shape and depth of the potential well show a strong dependence on the value of s. For negative spin values, such as $s = -0.8$, the potential well becomes significantly deeper and broader, indicating stronger gravitational binding. As the spin increases toward positive values, the depth of the well decreases, and the potential peak shifts inward, suggesting weaker binding and an enhanced repulsive effect due to spin-curvature coupling. The spinless case $s = 0$ lies between

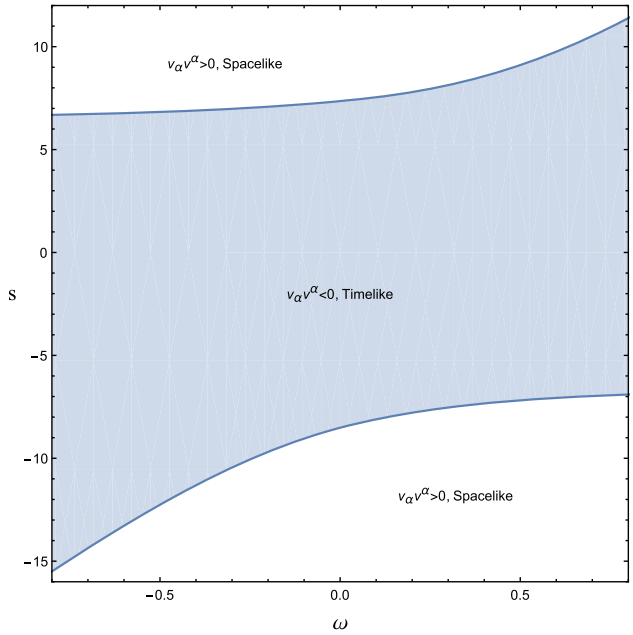

Fig. 1 Allowed regions in the (ω, s)-plane for a charged spinning particle around a magnetized Schwarzschild black hole. The shaded area corresponds to physically admissible (timelike) motion satisfying $v_\alpha v^\alpha < 0$, while the boundary curve marks the onset of superluminal behavior. The shape of the boundary reflects the nonlinear dependence of the superluminal limit on spin and magnetic interaction

these extremes and provides a useful reference configuration.

The right panel of Fig. 2 presents the effective potential for a fixed spin $s = 0.4$ and angular momentum $\mathcal{L} = 4$, while the magnetic coupling parameter ω is varied from -0.02 to 0.02. As ω increases, the potential becomes shallower and its minimum shifts outward, indicating that the magnetic interaction acts repulsively and reduces the particle's confinement. For negative values of ω, the potential well deepens and the minimum moves inward, reflecting enhanced attraction due to magnetic alignment with the black hole's field.

These results highlight the significant influence of both the spin and magnetic interaction on the particle's orbital behavior. A deeper potential well corresponds to more tightly bound orbits, while a shallower profile suggests reduced stability or even unbound motion. Therefore, by tuning the spin and magnetic coupling parameters, one can dramatically alter the dynamics of spinning test particles near magnetized black holes.

3.2 Innermost stable circular orbits

We now turn our attention to the circular motion of charged spinning test particles in the spacetime described by the Schwarzschild metric, given in Eq. (1). Circular orbits correspond to trajectories with constant radial coordinate, which implies that the radial velocity vanishes, $dr/d\lambda = 0$. Additionally, for a particle to remain in circular motion, its radial acceleration must also vanish, $d^2r/d\lambda^2 = 0$, which leads to the condition $dV_{\text{eff}}/dr = 0$.

However, these two conditions alone do not ensure orbital stability. For a circular orbit to be stable under small perturbations, the effective potential must have a local minimum, requiring the second derivative to be positive, $d^2V_{\text{eff}}/dr^2 > 0$. The boundary case where this derivative vanishes, $d^2V_{\text{eff}}/dr^2 = 0$, defines the innermost stable circular orbit (ISCO), which represents the smallest radius at which a stable circular orbit can exist.

By applying the conditions $\mathcal{E} = V_{\text{eff}}$ and $dV_{\text{eff}}/dr = 0$, one can determine the energy $\mathcal{E}$ and angular momentum $\mathcal{L}$ of the particle as functions of the orbital radius r. The ISCO condition $d^2V_{\text{eff}}/dr^2 = 0$ is then used to compute the

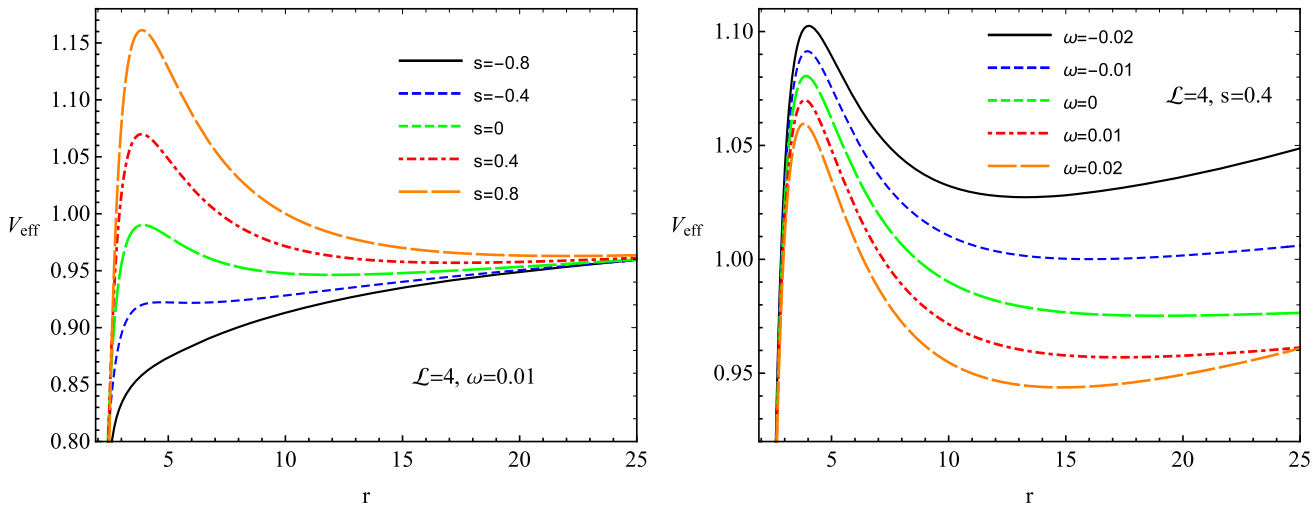

Fig. 2 Radial profiles of the effective potential for magnetized Schwarzschild black hole cases for different values of the test particle's spin s and ω parameter

limiting radius of stability for spinning particles. Since the resulting system of equations is nonlinear in r and $\mathcal{L}$, we solve it numerically and present the behavior of the solutions graphically.

In Fig. 3, we show the variation of the specific energy $\mathcal{E}_{\rm ISCO}$ (left panel), angular momentum $\mathcal{L}_{\rm ISCO}$ (middle panel), and the ISCO radius $r_{\rm ISCO}$ (right panel) of magnetized spinning particles as functions of the spin parameter s and magnetic coupling parameter ω. The top row of panels illustrates the dependence on the particle's spin s for selected values of magnetic coupling ω. As can be observed, increasing the spin parameter leads to a decrease in all three quantities — energy, angular momentum, and ISCO radius — particularly when ω is more negative. This trend reflects the enhanced binding effect and inward shift of the ISCO for spinning particles due to spin–magnetic coupling. The ISCO profiles become steeper as $s \to 2$, with the onset of sharp vertical changes indicating superluminal bounds, i.e., the maximum allowed spin before physical constraints are violated. This effect becomes more pronounced at stronger magnetic interactions.

The bottom row of Fig. 3 shows the same quantities as functions of ω for fixed spin values. As the magnetic coupling parameter increases from negative to positive values, the specific energy and angular momentum at the ISCO decrease for all spin cases, implying that stronger magnetic fields reduce the energy and torque required for stable circular motion. The ISCO radius, however, exhibits nonmonotonic behavior: for low spin, it increases slightly with ω and then decreases, while for higher spin values, the radius consistently decreases. This highlights the nontrivial interplay between magnetic confinement and spin-induced frame-dragging effects. The strongest decrease in $r_{\rm ISCO}$ with ω is observed for positive spin values, indicating that spin and magnetic effects act constructively to allow tighter, more efficient orbits closer to the black hole.

Overall, Fig. 3 demonstrates that both spin and magnetic coupling play crucial roles in shaping the energetics and geometry of circular particle motion. Higher spin and stronger magnetic interaction both favor deeper binding (lower $\mathcal{E}_{\rm ISCO}$), reduced angular momentum, and smaller ISCO radii. These findings are important for modeling accretion disk physics, particle trapping, and relativistic magnetohydrodynamics near compact objects in curved spacetime.

4 Collision of charged spinning particles

In this section, we study the center-of-mass energy $\mathcal{E}_{\rm cm}$ resulting from the collision of two charged spinning test particles in the background of a Schwarzschild black hole immersed in an external magnetic field. The particles are assumed to have equal rest mass, $m_1 = m_2 = m$, and interact both gravitationally and electromagnetically with the background spacetime through their spin and charge. The spin–curvature interaction is modeled using the Mathisson–Papapetrou–Dixon equations. At the same time, the electromagnetic coupling is introduced via a vector potential corresponding to a uniform test magnetic field aligned with the black hole's axis.

The covariant components of the particle momenta—p_t, p_ϕ, and p_r—are derived from the generalized momentum formalism, incorporating spin, charge, and magnetic interaction terms. These expressions, given explicitly in Eq. (30), provide the necessary input for computing dynamical quantities.

The center-of-mass energy of two colliding particles is computed using the general covariant formula:

$$\begin{aligned}\mathcal{E}_{\rm cm}^2 &= \frac{E_{\rm cm}^2}{2m^2} \\ &= 1 - g^{tt}u_t^{(1)}u_t^{(2)} - g^{t\phi}\left(u_t^{(1)}u_\phi^{(2)} + u_\phi^{(1)}u_t^{(2)}\right) \\ &\quad - g^{rr}u_r^{(1)}u_r^{(2)} - g^{\phi\phi}u_\phi^{(1)}u_\phi^{(2)},\end{aligned} \tag{36}$$

where $u_\mu^{(i)}$ are the covariant four-velocity components of the i-th particle, and $g^{\mu\nu}$ denotes the inverse components of the Schwarzschild metric.

Before analyzing $\mathcal{E}_{\rm cm}$ in detail, it is essential to determine the conditions under which a particle can approach the black hole. This leads to the concept of critical angular momentum – the maximum angular momentum that allows the particle to reach the horizon marginally. Inward motion requires $\dot{r}^2 \geq 0$, and the critical value is determined by the simultaneous equations $\dot{r}^2 = 0$ and $d\dot{r}^2/dr = 0$, corresponding to an extremum of the effective potential.

Figure 4 illustrates how the critical angular momentum varies with the spin parameter s and magnetic coupling ω. The left panel shows that increasing ω for fixed s raises the critical angular momentum, indicating that stronger magnetic interaction makes it more difficult for particles to fall into the black hole. This effect is particularly pronounced for negatively spinning particles, where spin-magnetic repulsion increases the threshold.

In the right panel, the critical angular momentum is plotted as a function of s for fixed ω. The dependence is nonmonotonic: it increases with s, peaks near $s \approx 0.8$, then declines. For high spin (e.g., $s = 1.8$), the magnetic interaction's influence fades and the critical angular momentum levels off, showing a balance between spin-induced attraction and magnetic repulsion.

Having established these threshold conditions, we now examine the radial behavior of $\mathcal{E}_{\rm cm}$ under different configurations. In Fig. 5, we present a parametric analysis in which the first particle's characteristics (s_1, $\mathcal{L}_1$, ω_1) are held fixed, while varying the second particle's properties.

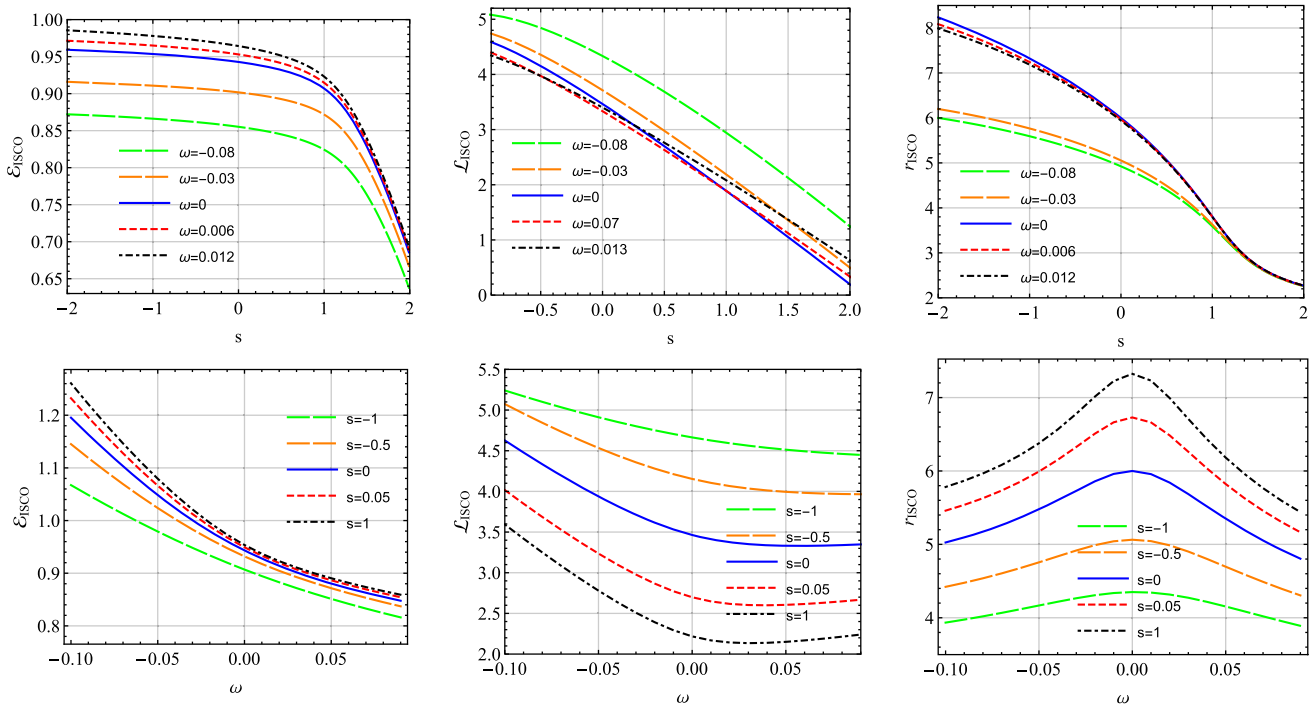

Fig. 3 Top row is for the dependencies of $\mathcal{E}_{\rm ISCO}$ (left panel), $\mathcal{L}_{\rm ISCO}$ (middle panel), and $r_{\rm ISCO}$ (right panel) on the particle's spin s for different values of the magnetic coupling parameter ω. Bottom row is for the dependencies of $\mathcal{E}_{\rm ISCO}$ (left panel), $\mathcal{L}_{\rm ISCO}$ (middle panel), and $r_{\rm ISCO}$ (right panel) on the magnetic coupling parameter ω for different values of the particle's spin s

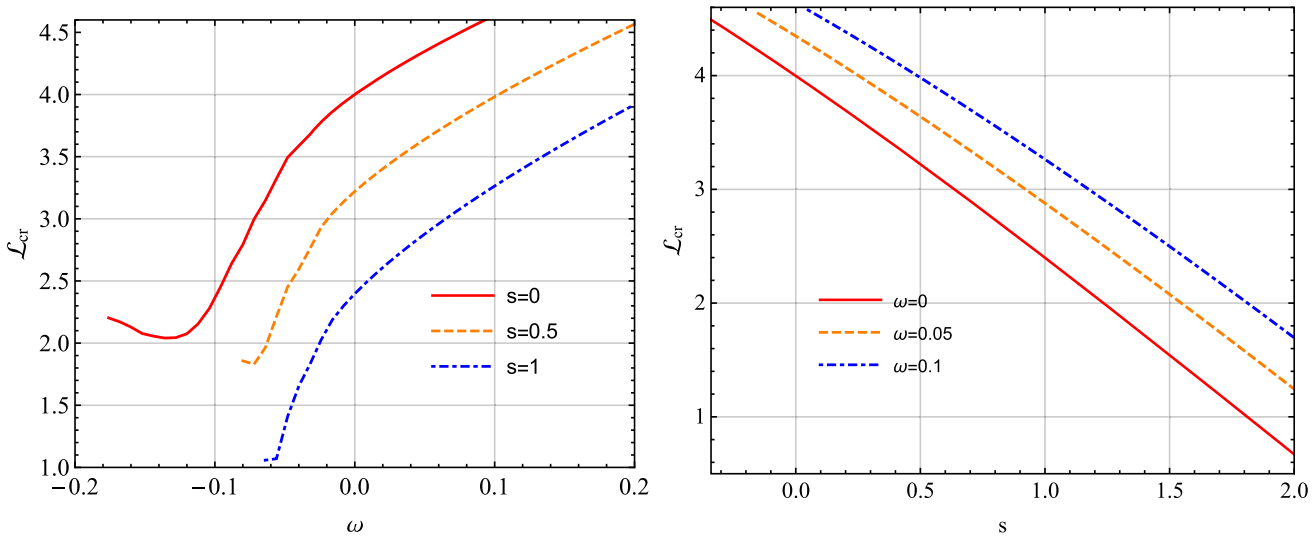

Fig. 4 Dependence of the critical angular momentum on the spin parameter s (left panel) and magnetic coupling parameter ω (right panel) for a charged spinning particle near a magnetized Schwarzschild black hole. Each curve corresponds to a fixed value of the other parameter

The top row of Fig. 5 shows that as ω_2 increases, $\mathcal{E}_{\rm cm}$ decreases. Stronger magnetic coupling for the second particle reduces the energy available at collision, especially when ω_1 is small. Energy enhancement is most notable near the horizon and diminishes with radius.

The middle row analyzes the spin s_2 of the second particle. Here, $\mathcal{E}_{\rm cm}$ decreases monotonically with s_2, consistent with suppressed relative motion from spin-curvature and spin-magnetic coupling. The drop is steepest at $s_2 = 1$.

Finally, the bottom row explores the effect of $\mathcal{L}_2$. Higher values of $\mathcal{L}_2$ lower the collision energy, confirming that counter-rotating configurations ($\mathcal{L}_2 < 0$) produce the most energetic encounters, especially when spin and orbital angular momentum are oppositely aligned.

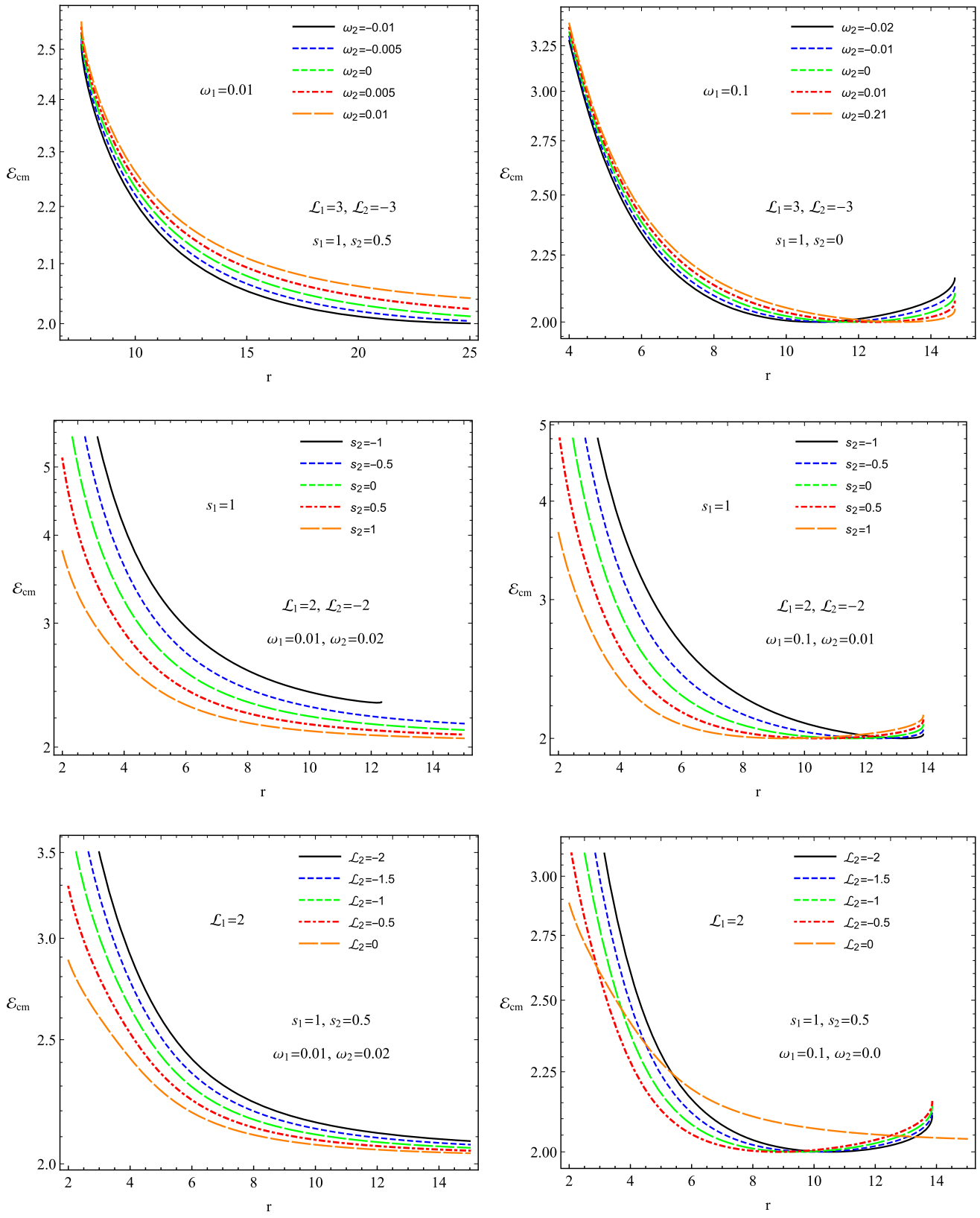

Fig. 5 Radial profiles of the center-of-mass energy $\mathcal{E}_{cm}$ for spinning charged particle collisions near a magnetized Schwarzschild black hole. Each panel illustrates different parameter configurations: varying ω_2 (top-left and top-right), s_2 (middle-left and middle-right), and $\mathcal{L}_2$ (bottom-left and bottom-right). Parameters s_1, $\mathcal{L}_1$, and ω_1 are kept fixed

These results highlight the interplay between spin, magnetic interactions, and orbital configurations in determining high-energy collisions near black holes. Understanding such mechanisms provides insight into energetic astrophysical processes in magnetized strong gravity regimes.

5 Conclusion

This study investigated the dynamics of charged spinning test particles orbiting a Schwarzschild black hole in the presence of an external magnetic field. By applying the Mathisson–Papapetrou–Dixon equations with the Tulczyjew SSC, we derived analytical expressions for the four-momentum and four-velocity, explicitly accounting for spin–magnetic coupling.

We analyzed the *superluminal bound*, a constraint ensuring that particles follow physically acceptable (timelike) trajectories. The resulting plots in the (ω, s)-plane revealed the precise spin ranges where causality is preserved. The boundary of these regions corresponds to critical spin values beyond which the particle's motion becomes unphysical (spacelike).

We also studied how spin and magnetic interactions affect the ISCOs. We found that increasing the spin can lower the ISCO radius and energy, enabling particles to orbit closer to the black hole stably. Furthermore, the presence of the magnetic field can either expand or restrict the allowed parameter space for circular motion, depending on the sign and magnitude of the spin.

Finally, we examined high-energy collisions of spinning particles and showed that favorable spin orientations and magnetic interaction can enhance the center-of-mass energy during collisions near the horizon. This suggests the possibility of extremely energetic events, relevant in astrophysical scenarios such as high-energy particle jets or radiation from accretion disks.

These findings emphasize how spin–magnetic interactions not only influence orbital stability but also impose fundamental physical limits on the motion of test particles in strong-field regimes.

Acknowledgements J.R. thanks Grant no. F-FA-2021-510 of the Uzbekistan Agency for Innovative Development. T.O. and J.R. acknowledge the Silesian University in Opava for warm hospitality.

Data Availability Statement This manuscript has no associated data. [Author's' comment: Data sharing not applicable to this article as no datasets were generated or analysed during the current study.]

Code Availability Statement This manuscript has no associated code/software. [Author's comment: Code/Software sharing not applicable to this article as no code/software was generated or analysed during the current study.]

Funded by SCOAP[3].

References

1. S. Gillessen, F. Eisenhauer, S. Trippe, T. Alexander, R. Genzel, F. Martins, T. Ott, Astrophys. J. **692**(2), 1075 (2009). https://doi.org/10.1088/0004-637X/692/2/1075
2. R. Genzel, F. Eisenhauer, S. Gillessen, Rev. Mod. Phys. **82**(4), 3121 (2010). https://doi.org/10.1103/RevModPhys.82.3121
3. E. Hackmann, C. Lämmerzahl, Y.N. Obukhov, D. Puetzfeld, I. Schaffer, Phys. Rev. D **90**(6), 064035 (2014). https://doi.org/10.1103/PhysRevD.90.064035
4. M. Mathisson, Gen. Relativ. Gravit. **42**(4), 1011 (2010). https://doi.org/10.1007/s10714-010-0939-y
5. A. Papapetrou, Proc. R. Soc. Lond. Ser. A **209**(1097), 248 (1951). https://doi.org/10.1098/rspa.1951.0200
6. E. Corinaldesi, A. Papapetrou, Proc. R. Soc. Lond. Ser. A **209**(1097), 259 (1951). https://doi.org/10.1098/rspa.1951.0201
7. W. Tulczyjew, Acta Phys. Pol. **18**(393), 94 (1959)
8. B. Tulzcyjew, W. Tulzcyjew, *Recent Developments in General Relativity*; Pergamon Press: New York, NY, USA, 1962
9. C. Møller, *On the Definition of the Centre of Gravity of an Arbitrary Closed System in the Theory of Relativity. Communications of the DIAS, Series A (Theoretical Physics) 5* (Dublin Institute for Advanced Studies, Dublin, 1949)
10. W. Beiglböck, Commun. Math. Phys. **5**(2), 106 (1967). https://doi.org/10.1007/BF01646841
11. W.G. Dixon, Il Nuovo Cimento **34**(2), 317 (1964). https://doi.org/10.1007/BF02734579
12. W.G. Dixon, Proc. R. Soc. Lond. Ser. A **314**(1519), 499 (1970). https://doi.org/10.1098/rspa.1970.0020
13. W.G. Dixon, Proc. R. Soc. Lond. Ser. A **319**(1539), 509 (1970). https://doi.org/10.1098/rspa.1970.0191
14. J. Ehlers, E. Rudolph, Gen. Relativ. Gravit. **8**(3), 197 (1977). https://doi.org/10.1007/BF00763547
15. W.G. Ramírez, A.A. Deriglazov, Phys. Rev. D **96**(12), 124013 (2017). https://doi.org/10.1103/PhysRevD.96.124013
16. A.A. Deriglazov, W.G. Ramírez, Phys. Lett. B **779**, 210 (2018). https://doi.org/10.1016/j.physletb.2018.01.063
17. J.M. Ladino, E. Larrañaga, Int. J. Mod. Phys. D **31**(12), 2250091 (2022). https://doi.org/10.1142/S0218271822500912
18. B. Toshmatov, D. Malafarina, Phys. Rev. D **100**(10), 104052 (2019). https://doi.org/10.1103/PhysRevD.100.104052
19. S. Shaymatov, B. Narzilloev, A. Abdujabbarov, C. Bambi, Phys. Rev. D **103**(12), 124066 (2021). https://doi.org/10.1103/PhysRevD.103.124066
20. J.M. Ladino, C. Andrés del Valle, E. Larrañaga, (2023). https://doi.org/10.48550/arXiv.2302.12352. arXiv e-prints arXiv:2302.12352
21. F. Abdulxamidov, C.A. Benavides-Gallego, W.B. Han, J. Rayimbaev, A. Abdujabbarov, Phys. Rev. D **106**(2), 024012 (2022). https://doi.org/10.1103/PhysRevD.106.024012
22. S. Shaymatov, P. Sheoran, S. Siwach, Phys. Rev. D **105**(10), 104059 (2022). https://doi.org/10.1103/PhysRevD.105.104059

23. F. Abdulxamidov, C.A. Benavides-Gallego, B. Narzilloev, I. Hussain, A. Abdujabbarov, B. Ahmedov, H. Xu, Eur. Phys. J. Plus **138**(7), 635 (2023). https://doi.org/10.1140/epjp/s13360-023-04283-9
24. J.M. Ladino, C.A. Benavides-Gallego, E. Larrañaga, J. Rayimbaev, F. Abdulxamidov, Eur. Phys. J. C **83**(11), 989 (2023). https://doi.org/10.1140/epjc/s10052-023-12187-2
25. F. Abdulxamidov, J. Rayimbaev, A. Abdujabbarov, Z. Stuchlík, Phys. Rev. D **108**(4), 044030 (2023). https://doi.org/10.1103/PhysRevD.108.044030
26. C.A. Benavides-Gallego, W.B. Han, D. Malafarina, B. Ahmedov, A. Abdujabbarov, Phys. Rev. D **104**(8), 084024 (2021). https://doi.org/10.1103/PhysRevD.104.084024
27. B. Toshmatov, O. Rahimov, B. Ahmedov, D. Malafarina, Eur. Phys. J. C **80**(7), 675 (2020). https://doi.org/10.1140/epjc/s10052-020-8254-6
28. T. Oteev, F. Abdulkhamidov, J. Rayimbaev, Z. Stuchlík, B. Ahmedov, Phys. Dark Universe **46**, 101588 (2024). https://doi.org/10.1016/j.dark.2024.101588
29. R.P. Eatough, H. Falcke, R. Karuppusamy, K.J. Lee, D.J. Champion, E.F. Keane, G. Desvignes, D.H.F.M. Schnitzeler, L.G. Spitler, M. Kramer, B. Klein, C. Bassa, G.C. Bower, A. Brunthaler, I. Cognard, A.T. Deller, P.B. Demorest, P.C.C. Freire, A. Kraus, A.G. Lyne, A. Noutsos, B. Stappers, N. Wex, Nature (London) **501**(7467), 391 (2013). https://doi.org/10.1038/nature12499
30. E.H.T. Collaboration, K. Akiyama, A. Alberdi, W. Alef, J.C. Algaba, R. Anantua, K. Asada, R. Azulay, U. Bach, A.K. Baczko, D. Ball, M. Balokovic, B. Bandyopadhyay, J. Barrett, M. Bauböck, B.A. Benson, D. Bintley, L. Blackburn, R. Blundell, K.L. Bouman, G.C. Bower, H. Boyce, M. Bremer, C.D. Brinkerink, R. Brissenden, S. Britzen, A.E. Broderick, D. Broguiere, T. Bronzwaer, S. Bustamante, D.Y. Byun, J.E. Carlstrom, C. Ceccobello, A. Chael, C.k. Chan, D.O. Chang, K. Chatterjee, S. Chatterjee, M.T. Chen, Y. Chen, X. Cheng, I. Cho, P. Christian, N.S. Conroy, J.E. Conway, J.M. Cordes, T.M. Crawford, G.B. Crew, A. Cruz-Osorio, Y. Cui, R. Dahale, J. Davelaar, M. De Laurentis, R. Deane, J. Dempsey, G. Desvignes, J. Dexter, V. Dhruv, I.K. Dihingia, S.S. Doeleman, S.T. Dougal, S.A. Dzib, R.P. Eatough, R. Emami, H. Falcke, J. Farah, V.L. Fish, E. Fomalont, H.A. Ford, M. Foschi, R. Fraga-Encinas, W.T. Freeman, P. Friberg, C.M. Fromm, A. Fuentes, P. Galison, C.F. Gammie, R. García, O. Gentaz, B. Georgiev, C. Goddi, R. Gold, A.I. Gómez-Ruiz, J.L. Gómez, M. Gu, M. Gurwell, K. Hada, D. Haggard, K. Haworth, M.H. Hecht, R. Hesper, D. Heumann, L.C. Ho, P. Ho, M. Honma, C.W.L. Huang, L. Huang, D.H. Hughes, S. Ikeda, C.M.V. Impellizzeri, M. Inoue, S. Issaoun, D.J. James, B.T. Jannuzi, M. Janssen, B. Jeter, W. Jiang, A. Jiménez-Rosales, M.D. Johnson, S. Jorstad, A.V. Joshi, T. Jung, M. Karami, R. Karuppusamy, T. Kawashima, G.K. Keating, M. Kettenis, D.J. Kim, J.Y. Kim, J. Kim, J. Kim, M. Kino, J.Y. Koay, P. Kocherlakota, Y. Kofuji, P.M. Koch, S. Koyama, C. Kramer, J.A. Kramer, M. Kramer, T.P. Krichbaum, C.Y. Kuo, N. La Bella, T.R. Lauer, D. Lee, S.S. Lee, P.K. Leung, A. Levis, Z. Li, R. Lico, G. Lindahl, M. Lindqvist, M. Lisakov, J. Liu, K. Liu, E. Liuzzo, W.P. Lo, A.P. Lobanov, L. Loinard, C.J. Lonsdale, A.E. Lowitz, R.S. Lu, N.R. MacDonald, J. Mao, N. Marchili, S. Markoff, D.P. Marrone, A.P. Marscher, I. Martí-Vidal, S. Matsushita, L.D. Matthews, L. Medeiros, K.M. Menten, D. Michalik, I. Mizuno, Y. Mizuno, J.M. Moran, K. Moriyama, M. Moscibrodzka, W. Mulaudzi, C. Müller, H. Müller, A. Mus, G. Musoke, I. Myserlis, A. Nadolski, H. Nagai, N.M. Nagar, M. Nakamura, G. Narayanan, I. Natarajan, A. Nathanail, S.N. Fuentes, J. Neilsen, R. Neri, C. Ni, A. Noutsos, M.A. Nowak, J. Oh, H. Okino, H. Olivares, G.N. Ortiz-León, T. Oyama, F. Özel, D.C.M. Palumbo, G.F. Paraschos, J. Park, H. Parsons, N. Patel, U.L. Pen, Astrophys. J. **964**(2), L25 (2024). https://doi.org/10.3847/2041-8213/ad2df0
31. Event Horizon Telescope Collaboration, K. Akiyama, A. Alberdi, W. Alef, J.C. Algaba, R. Anantua, K. Asada, R. Azulay, U. Bach, A.K. Baczko, D. Ball, M. Baloković, B. Bandyopadhyay, J. Barrett, M. Bauböck, B.A. Benson, D. Bintley, L. Blackburn, R. Blundell, K.L. Bouman, G.C. Bower, H. Boyce, M. Bremer, C.D. Brinkerink, R. Brissenden, S. Britzen, A.E. Broderick, D. Broguiere, T. Bronzwaer, S. Bustamante, D.Y. Byun, J.E. Carlstrom, C. Ceccobello, A. Chael, C.k. Chan, D.O. Chang, K. Chatterjee, S. Chatterjee, M.T. Chen, Y. Chen, X. Cheng, I. Cho, P. Christian, N.S. Conroy, J.E. Conway, J.M. Cordes, T.M. Crawford, G.B. Crew, A. Cruz-Osorio, Y. Cui, R. Dahale, J. Davelaar, M. De Laurentis, R. Deane, J. Dempsey, G. Desvignes, J. Dexter, V. Dhruv, I.K. Dihingia, S.S. Doeleman, S. Dougall, S.A. Dzib, R.P. Eatough, R. Emami, H. Falcke, J. Farah, V.L. Fish, E. Fomalont, H.A. Ford, M. Foschi, R. Fraga-Encinas, W.T. Freeman, P. Friberg, C.M. Fromm, A. Fuentes, P. Galison, C.F. Gammie, R. García, O. Gentaz, B. Georgiev, C. Goddi, R. Gold, A.I. Gómez-Ruiz, J.L. Gómez, M. Gu, M. Gurwell, K. Hada, D. Haggard, K. Haworth, M.H. Hecht, R. Hesper, D. Heumann, L.C. Ho, P. Ho, M. Honma, C.W.L. Huang, L. Huang, D.H. Hughes, S. Ikeda, C.M.V. Impellizzeri, M. Inoue, S. Issaoun, D.J. James, B.T. Jannuzi, M. Janssen, B. Jeter, W. Jiang, A. Jiménez-Rosales, M.D. Johnson, S. Jorstad, A.V. Joshi, T. Jung, M. Karami, R. Karuppusamy, T. Kawashima, G.K. Keating, M. Kettenis, D.J. Kim, J.Y. Kim, J. Kim, J. Kim, M. Kino, J.Y. Koay, P. Kocherlakota, Y. Kofuji, P.M. Koch, S. Koyama, C. Kramer, J.A. Kramer, M. Kramer, T.P. Krichbaum, C.Y. Kuo, N. La Bella, T.R. Lauer, D. Lee, S.S. Lee, P.K. Leung, A. Levis, Z. Li, R. Lico, G. Lindahl, M. Lindqvist, M. Lisakov, J. Liu, K. Liu, E. Liuzzo, W.P. Lo, A.P. Lobanov, L. Loinard, C.J. Lonsdale, A.E. Lowitz, R.S. Lu, N.R. MacDonald, J. Mao, N. Marchili, S. Markoff, D.P. Marrone, A.P. Marscher, I. Martí-Vidal, S. Matsushita, L.D. Matthews, L. Medeiros, K.M. Menten, D. Michalik, I. Mizuno, Y. Mizuno, J.M. Moran, K. Moriyama, M. Moscibrodzka, W. Mulaudzi, C. Müller, H. Müller, A. Mus, G. Musoke, I. Myserlis, A. Nadolski, H. Nagai, N.M. Nagar, M. Nakamura, G. Narayanan, I. Natarajan, A. Nathanail, S.N. Fuentes, J. Neilsen, R. Neri, C. Ni, A. Noutsos, M.A. Nowak, J. Oh, H. Okino, H. Olivares, G.N. Ortiz-León, T. Oyama, F. Özel, D.C.M. Palumbo, G.F. Paraschos, J. Park, H. Parsons, N. Patel, U.L. Pen, Astrophys. J., **964**(2), L26 (2024). https://doi.org/10.3847/2041-8213/ad2df1
32. U. Uktamov, M. Fathi, J. Rayimbaev, A. Abdujabbarov, Phys. Rev. D **110**(8), 084084 (2024). https://doi.org/10.1103/PhysRevD.110.084084
33. C.G.J. Jacobi, *Gesammelte Werke*, vol. 1 (G. Reimer, Berlin, 1881)
34. N.H. Abel, *Oeuvres complètes de Niels Henrik Abel* (Grøndahl & Søn, Christiania, 1881)
35. B. Riemann, Journal für die reine und angewandte Mathematik **54**, 115 (1857)
36. B. Riemann, Journal für die reine und angewandte Mathematik **65**, 161 (1866)
37. C. Weierstrass, Journal für die reine und angewandte Mathematik **47**, 289 (1854)
38. H.F. Baker, *Abel's Theorem and the Allied Theory, Including the Theory of the Theta Functions* (Cambridge University Press, Cambridge, 1897)
39. G.V. Kraniotis, S.B. Whitehouse, Class. Quantum Gravity **20**(22), 4817 (2003). https://doi.org/10.1088/0264-9381/20/22/007
40. G.V. Kraniotis, Class. Quantum Gravity **21**(19), 4743 (2004). https://doi.org/10.1088/0264-9381/21/19/016
41. N. Cruz, M. Olivares, J.R. Villanueva, Class. Quantum Gravity **22**(6), 1167 (2005). https://doi.org/10.1088/0264-9381/22/6/016
42. E. Hackmann, C. Lämmerzahl, Phys. Rev. Lett. **100**(17), 171101 (2008). https://doi.org/10.1103/PhysRevLett.100.171101
43. E. Hackmann, C. Lämmerzahl, Phys. Rev. D **78**(2), 024035 (2008). https://doi.org/10.1103/PhysRevD.78.024035

44. M.M. Suleimanov, M.U. Nosirov, H.T. Yusupov, A. Chaves, G.R. Berdiyorov, K.Y. Rakhimov, Phys. B **714**, 417484 (2025). https://doi.org/10.1016/j.physb.2025.417484
45. E. Hackmann, V. Kagramanova, J. Kunz, C. Lämmerzahl, EPL (Europhys. Lett.) **88**(3), 30008 (2009). https://doi.org/10.1209/0295-5075/88/30008
46. E. Hackmann, B. Hartmann, C. Lämmerzahl, P. Sirimachan, Phys. Rev. D **81**(6), 064016 (2010). https://doi.org/10.1103/PhysRevD.81.064016
47. M. Olivares, J. Saavedra, C. Leiva, J.R. Villanueva, Mod. Phys. Lett. A **26**(39), 2923 (2011). https://doi.org/10.1142/S0217732311037261
48. B. Hoseini, R. Saffari, S. Soroushfar, Class. Quantum Gravity **34**(5), 055004 (2017). https://doi.org/10.1088/1361-6382/aa5a63
49. M. Fathi, M. Olivares, J.R. Villanueva, Eur. Phys. J. C **80**(1), 51 (2020). https://doi.org/10.1140/epjc/s10052-020-7623-5
50. M. Fathi, M. Olivares, J.R. Villanueva, Eur. Phys. J. Plus **136**(4), 420 (2021). https://doi.org/10.1140/epjp/s13360-021-01441-9
51. M. Fathi, M. Olivares, J.R. Villanueva, Eur. Phys. J. C **81**(11), 987 (2021). https://doi.org/10.1140/epjc/s10052-021-09787-1
52. M. Fathi, M. Olivares, J.R. Villanueva, Eur. Phys. J. Plus **138**(1), 7 (2023). https://doi.org/10.1140/epjp/s13360-022-03538-1
53. M. Akramov, C. Trunk, J. Yusupov, D. Matrasulov, EPL (Europhys. Lett.) **147**(6), 62001 (2024). https://doi.org/10.1209/0295-5075/ad752e
54. B. Turimov, S. Usanov, Phys. Lett. B **867**, 139617 (2025). https://doi.org/10.1016/j.physletb.2025.139617
55. M. Fathi, Ann. Phys. **457**, 169401 (2023). https://doi.org/10.1016/j.aop.2023.169401
56. L. Perek, Vistas Astron. **5**(1), 28 (1962). https://doi.org/10.1016/0083-6656(62)90003-X
57. M. Barbieri, R.G. Gratton, Astron. Astrophys. **384**, 879 (2002). https://doi.org/10.1051/0004-6361:20020011
58. Y.P. Zhang, S.W. Wei, Y.X. Liu, Universe **6**(8), 103 (2020). https://doi.org/10.3390/universe6080103
59. R.M. Wald, *General Relativity* (University of Chicago Press, Chicago, 1984)
60. Z. Stuchlík, M. Kološ, J. Kovář, P. Slaný, A. Tursunov, Universe **6**(2), 26 (2020). https://doi.org/10.3390/universe6020026
61. Z. Stuchlík, M. Kološ, A. Tursunov, Universe **7**(11), 416 (2021). https://doi.org/10.3390/universe7110416
62. D. Umarov, F. Atamurotov, S.G. Ghosh, A. Abdujabbarov, G. Mustafa, Eur. Phys. J. C **85**(7), 800 (2025). https://doi.org/10.1140/epjc/s10052-025-14541-y
63. H.Z.C. Liu, S. Chen, Universe **6**(8), 103 (2020)
64. O.B. Zaslavskii, Phys. Rev. D **103**, 124066 (2021)
65. A.A.L. Benavides-Gallego, B. Ahmedov, Eur. Phys. J. C **81**, 660 (2021)
66. R. Hojman, S. Hojman, Phys. Rev. D **15**(10), 2724 (1977). https://doi.org/10.1103/PhysRevD.15.2724
67. M. Saijo, K.I. Maeda, M. Shibata, Y. Mino, Phys. Rev. D **58**, 064005 (1998). https://doi.org/10.1103/PhysRevD.58.064005
68. M. Saijo, K.I. Maeda, M. Shibata, Y. Mino, Phys. Rev. D **58**(6), 064005 (1998). https://doi.org/10.1103/PhysRevD.58.064005
69. M.D. Ramírez, A.A. Deriglazov, Phys. Rev. D **104**(2), 024042 (2021). https://doi.org/10.1103/PhysRevD.104.024042
70. A. Ohashi, K. Kyrian, O. Semerák, Phys. Rev. D **108**(6), 064050 (2023). https://doi.org/10.1103/PhysRevD.108.064050
71. C. Conde, C. Galvis, E. Larrañaga, Phys. Rev. D **99**(10), 104059 (2019). https://doi.org/10.1103/PhysRevD.99.104059
72. S.A. Hojman, F.A. Asenjo, Class. Quantum Gravity **30**(2), 025008 (2013). https://doi.org/10.1088/0264-9381/30/2/025008